Standoff ultra-compact μ-Raman sensor for planetary surface explorations

M. NURUL ABEDIN[1], ARTHUR T. BRADLEY[1], ANUPAM K. MISRA[2], YINGXIN BAI[3], GLENN D. HINES[1], AND SHIV K. SHARMA[2].

[1]NASA Langley Research Center, Hampton, VA 23681
[2]University of Hawaii at Manoa, Honolulu, Hawaii 96822
[3]Science Systems and Applications, Inc., Hampton, VA 23666

We report the development of an innovative Standoff Ultra-Compact micro-Raman (SUCR) instrument that would solve some of the limitations of traditional micro-Raman systems to provide a superior instrument for future NASA missions. This active remote sensor system, based on a 532 nm laser and a miniature spectrometer, is capable of inspection and identification of minerals, organics, and biogenic materials within several centimeters (2 to 20 cm) at a high 10 micrometer resolution. The sensor system is based on inelastic (Raman) light scattering and Laser-Induced Fluorescence (LIF). We report on micro-Raman spectroscopy development and demonstration of the standoff Raman measurements by acquiring Raman spectra in daylight at a 10 cm target distance with a small line-shaped laser spot size of 17.3 micrometer (width) by 5 millimeter (height).

1. INTRODUCTION

An increasing interest in implementation of Raman spectroscopy is observed due to its spectral sharpness and precise detection of specific species, especially in the presence of complex mixtures. Raman spectra consist of a variety of molecular fingerprint information that make this technique very attractive to the planetary science community to investigate planetary materials. This technique can be used to identify water containing minerals, biomarkers, biominerals, minerals, and chemical compounds based on the positions of vibrational frequencies, relative intensities, band widths, and number of Raman lines in the spectra [1-6]. Crystalline polymorphs [7-8], amorphous vs. crystalline ices, and clathrates [9-13] were investigated using this Raman detection technique due to its unequivocal inspection capability.

The search for life on other planets and other Solar System objects is one of the important goals outlined in the NASA Decadal Survey 2013-2022 [14]. To date, there has been no evidence that life exists outside of Earth. However, the detection of biological materials and biomarkers would be evidence in support of life outside our planet and an important step towards meeting the goals of the NASA Planetary Exploration Program.

Raman spectroscopy, as one of its strengths, can be used to detect the presence of life. Signs of life forms past or present can be realized through the detection of specific biomarkers, such as amino acids, whether life is extant or extinct. These amino acids, the ‘building-blocks’ of proteins, have been

identified as a high priority biomarker in the search for evidence of life on planetary bodies [15] and are part of a biological system that could provide potential evidence of life on Mars. Raman spectroscopy is also a powerful technique for characterizing and analyzing geological samples as well as biological molecules, and has been suggested as a detection technique for biomarkers on missions to planetary bodies [16]. Edwards et al. [17] and Jehlicka et al. [18] have successfully investigated Raman spectroscopy to detect organics and biomarkers for exobiological applications.

The case for a micro-Raman instrument has been identified in the recent Mars 2020 Science Definition Team (SDT) final report [19]. There are two micro-Raman systems under development for future missions: the Raman Laser Spectrometer (RLS) for Exo-Mars (2018) [20-22] and Mars Micro-beam Raman Spectrometer (MMRS) by JPL and the University of Washington (UW) [23]. Current micro-Raman instruments have some limitations: they are slow to generate a Raman image and they require sample collection. By understanding the limitations of current micro-Raman systems, it becomes obvious that there is a strong need for the development of a more sensitive and faster system for NASA exploration programs. Here we discuss how to solve some of these limitations by developing a new compact Standoff Ultra-Compact Raman (SUCR) instrument for future NASA missions for rapid daytime mineralogy and micro-Raman imaging without sample collection.

2. EXISTING MICRO-RAMAN SYSTEMS AND THEIR LIMITATIONS

Micro-Raman systems are developed for planetary rovers for *in situ* analysis. In order to determine whether life ever evolved on Mars, the European Space Agency (ESA) expects to launch an exobiology mission known as Exo-Mars to Mars in 2018. As part of ESA's long-term Aurora program to prepare for future human missions, Exo-Mars will deploy a high-mobility rover on the Martian surface. The RLS, one part of the Pasteur instrument payload, is a micro-Raman system. RLS has two main objectives: identify organic compounds in the search for life and identify the mineral products or other indicators of biological activities [20-21]. Similarly, JPL and the University of Washington have developed a MMRS micro-Raman system [23]. Both MMRS and RLS micro-Raman systems use a Continuous Wave (CW) 532 nm laser for Raman excitation. Light is transferred from the collecting optics to the spectrographs using a fiber optic cable. The spectrographs utilize transmission gratings and Charge-Coupled Device (CCD) detectors to record the Raman spectra, which is incapable of performing time-resolved measurements. Because of this traditional approach, these micro-Raman systems have the following limitations: (i) they require sample collection and manipulation, (ii) they cannot operate in daylight conditions, (iii) they are affected by the presence of mineral luminescence, and (iv) they are slow for generating Raman images.

These limitations significantly lower the science return in terms of the number of samples that can be analyzed in a day from a micro-Raman system, mostly due to the need for sample collection, sample manipulation of proper focusing distance, and complete shielding of daylight background. Under the current Exo-Mars mission, samples will be crushed into powders and then presented to the RLS chamber [20]. MMRS will only collect data during the Mars early night [23].

These micro-Raman systems are slow and most of the Raman spectra collected by MMRS have a typical integration time of 60 seconds [23]. Similarly, RLS has measured a bulk calcite sample using integration times ranging from 3 to 12 seconds [22]. This will translate into a very long interrogation time needed to generate a Raman chemical map.

The slow speed for generating Raman imaging is a known problem in the Raman spectroscopy community.

3. DEVELOPMENT METHODOLOGY

The working principle of the SUCR system is based on a directly coupled remote Raman system that obtains high quality Raman spectra of distant targets in daytime with very short integration times. To develop the SUCR, we modified the collecting optics for acquiring micro-Raman spectra at several centimeters distance, implemented vertical line imaging for faster Raman images, further miniaturized the Raman spectrometer, and improved vertical imaging resolution to around 10 microns.

Raman spectroscopy is typically envisioned as an *in situ* analysis technique. The potential for performing Raman analysis remotely was explored theoretically as early as 1974 by Hirschfeld [24] and experimentally in the 1990s [25-26]. At NASA LaRC, Abedin et al. [27-28] and the University of Hawaii, Sharma et al. [29-38] and Misra et al. [39-44] measured remote Raman spectra of minerals and organic compounds up to 15-120 m away. These remote Raman systems provide high quality Raman spectra from a distance, in daytime, without sample collection, and with rapid speed. Recently the Univ. of Hawaii demonstrated good quality, remote Raman detection of several minerals from a distance of 430 m and with 1 s integration time in the afternoon with the Sun shining on the targets [45]. The SUCR provides these same capabilities as larger systems, but on a microscopic scale. With a short working distance of several centimeters there is a significant increase in the signal and significant decrease in the size of the Raman system. A high power laser and a large collection lens are not needed at short distances. Therefore, we can further miniaturize the collection optics, spectrograph, and laser optics of our already compact remote Raman system developed at NASA LaRC and the University of Hawaii, further reducing the size and weight of the SUCR instrument.

Our SUCR instrument uses pulsed-time gated Raman technology capable of operating in daylight. This provides a superior micro-Raman instrument for future NASA missions. A block diagram and a 3-D enclosure design of the SUCR system are shown in Figure 1. This consists of a transmitter and a spectrograph.

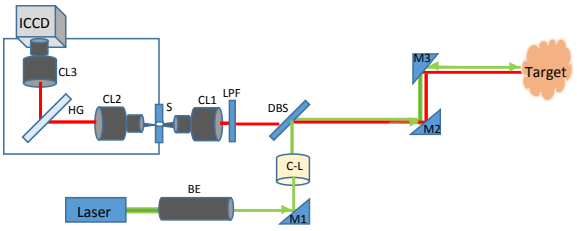

(a) Block Diagram of SUCR instrument

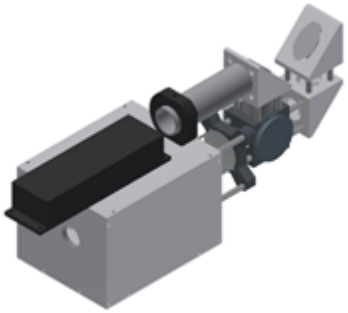

(b) 3-D Enclosure Design

Figure 1. Block diagram of SUCR instrument system (a) and the 3-D enclosure design of the system (b).

The key components of this transmitter and spectrograph are a compact Nd: YAG laser from CrystaLaser, which transmits at a 532 nm pulse with a total laser energy of 50 μJ/pulse, and a 10 ns pulse width at a repetition rate of 1.0 kHz. The laser beam transmits through a 532 nm dichroic filter to the target surface. The backscatter signals are received by the collection optics and pass to the spectrograph through a notch filter or a long pass filter and a slit. The long pass filter (LPF) was used in this work to reflect or block the 532 nm laser line

from the wave trains. The Raman signals pass through focusing optics and an ultra-compact volume phase grating spectrograph to a mini Intensified Charge-Coupled Device (ICCD) camera. This ICCD camera detects signals in the 534 nm to 700 nm spectral range through the spectrograph, which covers the entire Raman spectral range.

4. Line-Shaped LASER SPOT SIZE 10 μm X 5 mm DEMONSTRATION

We report the development of a pulsed line scan image Raman spectrometer. The resolution for line-shaped laser excitation is 10 μm as discussed in Figure 2. First, we performed an optical ray trace simulation, as seen in Figure 2, to get the quantitative analysis of the beam size. To achieve a laser beam size of 10 μm by 5 mm, the laser beam from the CrystaLaser passed through the beam expander to make a collimated beam with a 5 mm beam diameter. A cylindrical lens with a focal length of 60 mm was used to reduce the beam size from 5 mm to around 10 μm at a target distance of 6 cm. To characterize the beam size, we used the well-known knife edge technique to measure the laser beam's properties including beam waist, divergence angle, and beam quality. Based on the parameters of a laser beam, we designed the laser illumined system and Raman image system. Both of the systems are coaxial which makes the system insensitive to variation in the target distance [39]. The coaxial geometry of the directly coupled Raman system has a large sampling range in comparison to a fiber coupled system. This eliminated the need for a precise working distance between the target and the system. This also helped in analyzing 3-D objects with a rough surface morphology. We selected the cylindrical lens with a 60 mm focal length (in Fig. 2) and characterized the beam size at a 6 cm target distance with a 10 μm x 5 mm spot size. Other spot sizes were determined using the following equation, $\omega o = \frac{M^2.\lambda}{\pi.\theta}$ (where ωo is the radius of the laser beam at the beam waist, λ is the laser wavelength, M^2 is quality of the beam, and θ is the divergence half angle in radian) at different locations with different cylindrical lenses. Cylindrical lenses with effective focal lengths of 60 mm, 100 mm, and 200 mm, were used. They provided beam spots of 10 μm x 5 mm, 17.3 μm x 5 mm, and 33.5 μm x 5 mm on the target distances at 60 mm, 100 mm, and 200 mm, respectively.

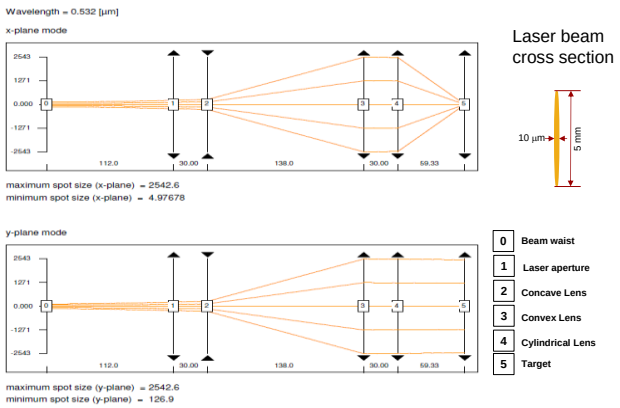

Figure 2. Laser beam determination: x-plane mode shows 10 μm beam width and y-plane mode shows 5 mm length.

5. μ-RAMAN SYSTEM PERFORMANCE DEMONSTRATION

In this study, special consideration was given to further miniaturize the size and weight of the instrument. At a short working distance, the Raman signal was expected to be significantly larger because of $1/R^2$ dependence (R is target range) of signal intensity. This allowed for significant reduction in the size of both the excitation laser and the collection optics, hence, we built the SUCR system for planetary exploration. Figure 3(a) shows the SUCR instrument in a 3-D enclosure. Figure 3(b) shows a grating, a c-mount lens and a slit inside the spectrograph, and Figure 3(c) shows a SUCR instrument system with mounting optical components, an ICCD, and a laser. The target distance from the collecting optics is ~10 cm, which was determined through a ray trace design in Figure 2 using a 532 nm laser with

0.05 mJ energy at a 1 kHz repetition rate (see Fig. 3(a, c)). The SUCR system can be used as a hand-held instrument to characterize and identify unknown samples and interpret them in real time.

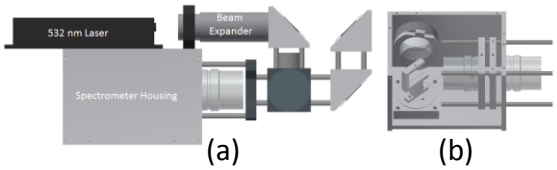

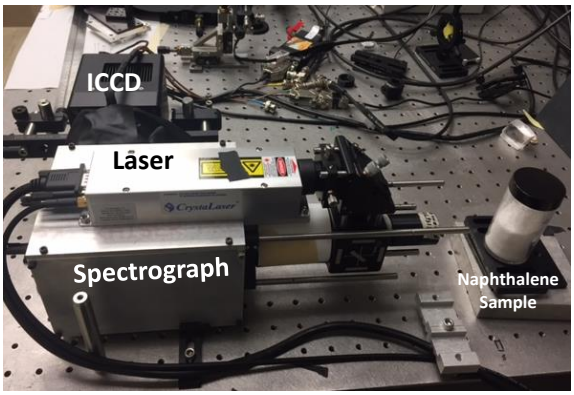

Figure 3. Stand-off Ultra-Compact Instrument design shows a 3-D enclosure in (a), a grating, c-mount lens and a slit inside spectrograph in (b), and mounting optical components, an ICCD, a laser, and a target naphthalene sample at a 10 cm target distance in (c).

The system operates in both daytime and nighttime conditions and is not restricted by background noise. The mini-ICCD consumes 3.5 W with Peltier cooling. The total energy consumption of the sensor is low because of the fast data collection. For a 20 cm target range, the total data collection time to collect a Raman line image of size ~34 micron x 5 mm is 0.1 second. The commercially available compact Q-Switch pulsed laser from CrystaLaser operating at 1 kHz weighs 600 g and consumes 40 W.

This miniaturized version of the Raman spectrometer (16.5 cm (length) x 11.4 cm (width) x 12.7 cm (height)) was constructed using a custom HoloPlex grating from Kaiser Optical Systems, Inc. (KOSI). The mass of the spectrograph with optics and laser from CrystaLaser is 4.6 kg. The miniaturized spectrograph is based on a custom HoloPlex grating from KOSI and covers the spectral range of 100 cm^{-1} to 4500 cm^{-1} (534 - 699.5 nm), Stokes-Raman shifted from the 532 nm laser excitation line. The SUCR system shown in Fig. 3(c) utilizes a regular 25.4 mm diameter lens as the collection optics. The SUCR was tested to measure Raman spectra of sulfur, naphthalene, mix samples (naphthalene + sulfur), marble, water, calcite minerals, and amino acids from 10 cm with a room light on. We report Raman spectra of sulfur, naphthalene, mix samples, water, calcite, and amino acids (L-glutamine) at a 10 cm target distance with a 17.3 µm x 5 mm laser spot in this article. The luminescence spectra of ruby is also presented to demonstrate spectral resolution of the system.

6. RESULTS AND DISCUSSION

We report standoff spectra of ruby, sulfur, naphthalene, combined naphthalene and sulfur, water, calcite, and amino acids using the above-mentioned spectrometer at a distance of 10 cm as shown in Figures 4 to 8. Figure 4 shows the luminescence spectra of ruby using continuous wave (CW) mode of the system. The strongest phosphorescence bands are produced by the Cr^{3+} phosphorescence R1 and R2 doublet. The doublet has very strong and sharp lines at 693 nm and 694 nm [34, 46-47]. A broad band in the 653 – 676 nm of the ruby is easily distinguishable. Figure 4 shows the capability of the compact spectrograph to resolve ruby lines demonstrating high spectral resolution.

Figures 5a, 5b, and 5c show the Raman spectra of sulfur, naphthalene (low and high frequency regions), and combined sulfur and naphthalene (low frequency region), respectively, employing gate widths of 150 ns. Identifiable Raman lines were observed at this gate width as seen in both naphthalene and sulfur spectra. The Raman spectra of sulfur in

Figure 5a are measured and the characteristic features are due to the vibrational modes of the sulfur sample. The sharp and narrow Raman fingerprints are detected at 85, 155, 220, 439, and 476 cm^{-1} for the low frequency region [34]. The Raman spectra of naphthalene in 5b are measured and the characteristic peaks are 109, 514, 765, 896, 1022, 1149, 1382, 1464, 1577, and 1628 for the low frequency and 3058 cm^{-1} for the high frequency regions (5b and 5c) [39, 48-49]. Similarly, Raman spectra of combined samples are obtained and displayed in Fig. 5d. Results in Fig. 5d are compared with the results obtained by combining individual Raman spectra of naphthalene and sulfur (Figs. 5b and 5c), which match very well.

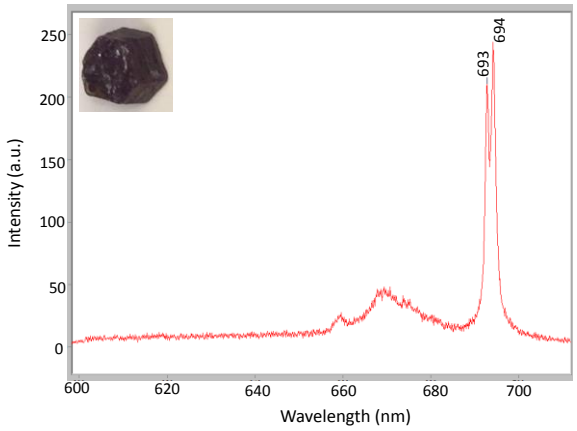

Figure 4. Luminescence spectra of ruby at a 10 cm distance with CW mode.

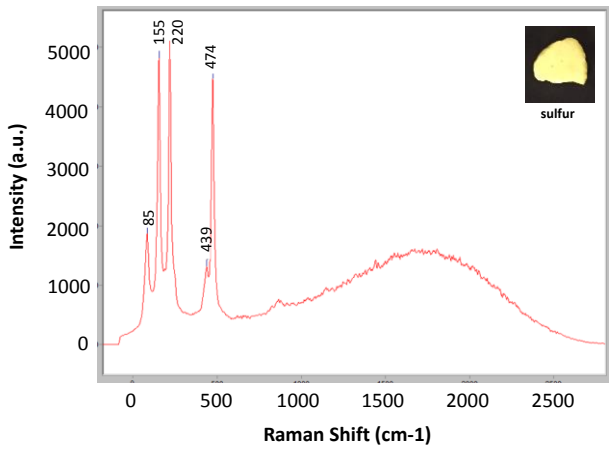

(a)

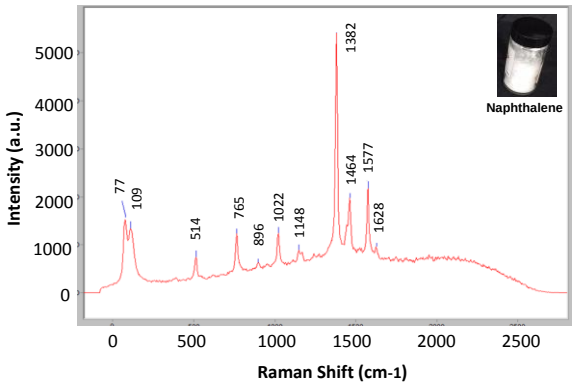

(b)

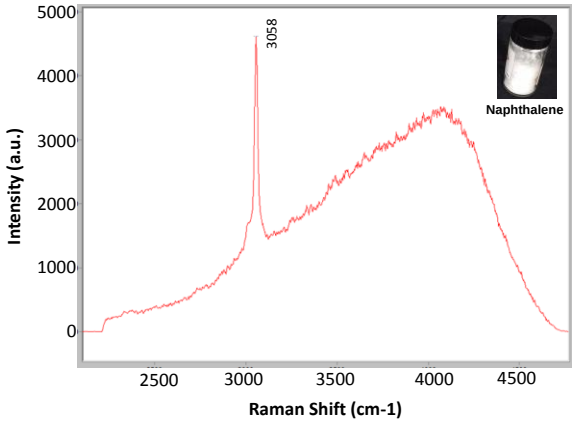

(c)

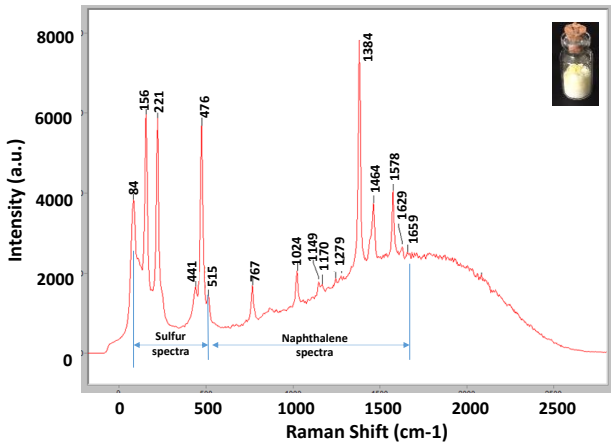

(d)

Figure 5. Raman spectra of sulfur and naphthalene ((a), (b) low frequency and (c) high frequency and combined spectra in ((d) low frequency) at a 10 cm target distance. 532 nm laser with energy 50 µJoule and 1 kHz repetition rate.

Figure 6 depicts the high frequency region in the Raman spectra of water obtained with the SUCR system. This Raman sensor system has been demonstrated to have an excellent ability to measure the symmetric and antisymmetric stretching O-H vibrational modes of water molecules that can be found in the 3100-3600 cm^{-1} region of their Raman spectra, as can be seen in Figure 6 in the spectra of water [43].

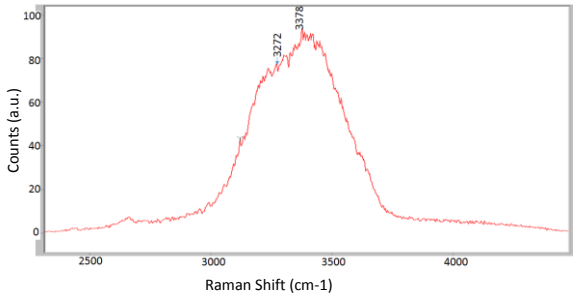

Fig. 6. High frequency Raman spectra of liquid water.

The Raman spectra of mineral calcite are shown in the low frequency region in Figure 7. These spectra were obtained using a 150 ns gate width and an integration time of 1.57 s. The low frequency spectra show a few sharp peaks at around 156, 282, 712, 1084, 1435, and 1748 cm^{-1} [34, 39, 50]. These are due to the vibrational modes of $CaCO_3$ structure.

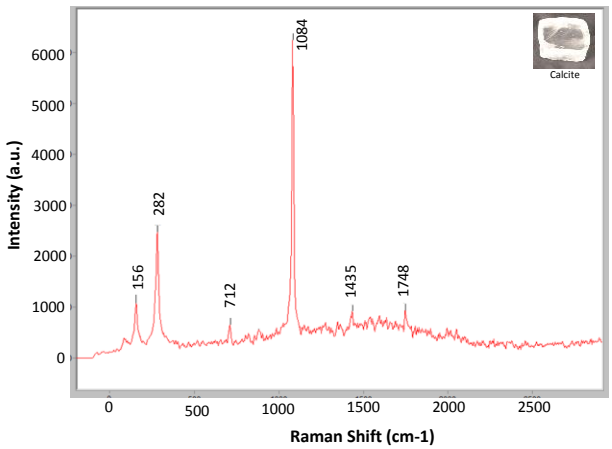

Fig. 7. Low frequency Raman spectra of mineral calcite.

Figure 8 shows the Raman spectra of amino acid L-glutamine, which was placed at the target distance of 10 cm. Figure 8 (a) shows the low frequency spectral range between 100 - 2600 cm^{-1}. The low frequency range is considered the fingerprint region of the amino acid glutamine. Raman peaks of L-glutamine were determined and compared to the published results in ref. 52. The low frequency Raman spectra show sharp peaks at 1642, 1604, 1497, 1169, and 1136 as the NH_3^+ rocking vibrations and the sharp peak at 1099 cm^{-1} as the NH_2 rocking vibrations [52]. The Raman sharp peaks at 1685 and 1621 cm^{-1} are due to the C=O and CO_2 stretching modes, and the peaks at 1450 and 1420 cm^{-1} are due to the CH_2 vibrations. Figure 8 (b) shows the high frequency spectral range between 2600 - 4500 cm^{-1} for the amino acid glutamine. The bands between 2887 and 3200 cm^{-1} are due to C–H stretching [51, 52, and 53]. The high frequency Raman spectra show sharp peaks at 3406 and 3202 cm^{-1}, which are due to the NH_2 stretching symmetric vibrations; and the Raman peaks at 3174, 2990, 2958, and 2935 that are due to the CH_2 and CH stretching vibrations [52]. The detected sharp peaks are assigned as rocking vibrations, stretching modes, etc., in addition, further peak assignments and their discussion are provided in ref. 52, too.

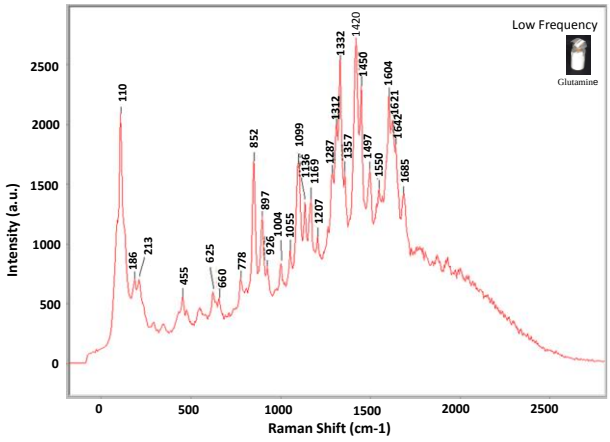

(a)

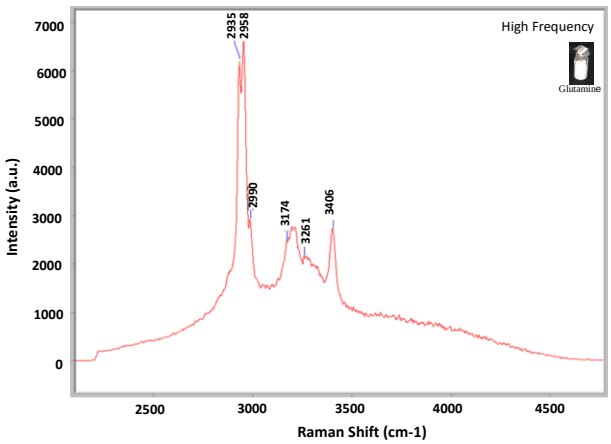

(b)

Fig. 8: Standoff Raman spectra of amino acid, L-glutamine, in low frequency (a) and high frequency regions at 10 cm distance.

7. CONCLUSION

In summary, we have presented Raman spectra minerals, organics, biogenic amino acids and water samples from a 10 cm distance using a newly developed standoff ultra-compact micro-Raman system with 17.3 µm resolution. The Raman spectra were measured through sealed glass vials and with all room lights turned on using nano-second pulsed gating. The luminescence spectra of ruby is shown to demonstrate high spectral resolution of the compact spectrograph. Development of this compact, sensitive, and faster Raman systems would be highly suitable for future NASA exploration programs aiming to detect evidence of life on other planets.

Funding

This research study was supported in part by a joint NASA Planetary Instrument Concepts for the Advancement of Solar System Observations (PICASSO) Project awarded to NASA LaRC and the University of Hawaii.

REFERENCES

1. S.K. Sharma, (1989) Applications of advanced Raman techniques in earth sciences. *Vibrational Spectra and Structure*, **17B**, 513-568.
2. A. Wang, J. Han, L. Guo, J. Yu, and P. Zeng (1994) Database of stand Raman spectra of minerals and related inorganic crystals, *Appl. Spectroscopy*, **48**, 959-968.
3. A. Wang, B.L. Jolliff, and L.A. Haskin (1995) Raman spectroscopy as a method for mineral identifications on lunar robotic exploration missions. *J. Geophys. Res.* **100**, 21189-21199.
4. I.A. Degen and G.A. Newman (1993) Raman spectra of inorganic ions. *Spectrochim. Acta*, **49**, 859-887.
5. P.F. McMillan and A.M. Hofmeister (1988) Crystal lattice vibrations. In F. C. Hawthorne (ed.), *Reviews in Mineralogy: Spectroscopic Methods*, **18**, pp. 103-105.
6. K. Nakamoto (1997) Infrared*and Raman Spectra of Inorganic and Coordination Compounds*, 5th edition. John Wiley and Sons, New York.
7. R.W. Gauldie, S.K. Sharma and E. Volk (1997) Micro-Raman spectra of Vaterite and Aragonite otoliths of Coho Salmon, *Oncorhynchuskisutch*. *Comp. Biochem. Physiol.*, **119A,** 753-757.
8. S.K. Sharma and J.P. Urmos (1987) Micro-Raman spectroscopic studies of materials at ambient and high pressures with CW and pulsed lasers. In Roy H. Geiss (ed.), *Microbeam Analysis - 1987*, pp. 133-136, San Francisco Press Inc.
9. M.J. Taylor and E. Whalley (1964) Raman spectra of ices Ih, Ic, II, II, and V. *J. Chem. Phys.* **40**, 1660-1664.
10. H.-C. Cynn, S. Boone, A. Koumvakalis, M. Nicol, and D. J. Stevenson 1989. Phase diagram for ammonia-water mixtures at high pressures: Implications for icy satellites, *Proc. Lunar Planet. Sci. Conf. 19th*, Lunar and Planetary Institute, Houston.
11. J.P. Devlin (1989) Polarized Raman spectra for the full range of isotopic dilution for ice

IC and amorphous ice: Mixtures of intact H_2O and D_2O. *J. Chem. Phys.* **90**, 1322-1329.

12. F. Pauer and J. Kipfstuhl (1995) Raman spectroscopic study on the nitrogen/oxygen ratio in natural ice clathrates in the GRIP ice core. *Geophys. Res. Lett.* **22**, 969-971.

13. S.K. Sharma, A. K. Misra, and B. Sharma (2005a) Portable remote Raman system for monitoring hydrocarbon, gas hydrates and explosives in the environment, *SpectrochimActa* A **61**, 2404-2412.

14. National Research Council, Committee on the Planetary Science Decadal Survey, Vision and Voyages for Planetary Science in the Decade 2013-2022, National Academic Press, Washington, 382 pp, 2011.

15. J. Parnell, D. Cullen, M.R. Sims, S. Bowden, et al., Searching for Life on Mars: Selection of Molecular Targets for ESA's Aurora ExoMars Mission. Astrobiology, 7(4): p. 578-604 (2007).

16. J. Jehlicka, H.G.M. Edwards, and P. Vítek, Assessment of Raman spectroscopy as a tool for the non-destructive identification of organic minerals and biomolecules for Mars studies. Planetary and Space Science, 2009. 57(5-6): p. 606-613.

17. H.G.M. Edwards, I. Hutchinson, and R. Ingley (2012) The ExoMars Raman spectrometer and the identification of biogeological spectroscopic signatures using a flight-like prototype, *Anal Bioanal Chem* **404**,1723–1731.

18. J. Jehlicka, H.G.M. Edwards, A. Culka (2010) Using portable Raman spectrometers for the identification of organic compounds at low temperatures and high altitudes: exobiological applications, *Phil. Trans. R. Soc.*A 368, 3109–3125.

19. J.F. Mustard, M. Adler, A. Allwood, D.S. Bass, D.W. Beaty, J.F. Bell III, W.B. Brinckerhoff, M. Carr, D.J. Des Marais, B. Drake, K.S. Edgett, J. Eigenbrode, L.T. Elkins-Tanton, J.A. Grant, S. M. Milkovich, D. Ming, C. Moore, S. Murchie, T.C. Onstott, S.W. Ruff, M.A. Sephton, A. Steele, A. Treiman (2013): Report of the Mars 2020 Science Definition Team, 154 pp., posted July, 2013, by the Mars Exploration Program Analysis Group (MEPAG) at http://mepag.jpl.nasa.gov/reports/MEP/Mars_2020_SDT_Report_Final.pdf.

20. F. Rull, A. Sansano, E. Díaz, C.P. Canora, A.G. Moral, C. Tato, M. Colombo, T. Belenguer, et al., (2011a), ExoMars Raman Laser Spectrometer for Exomars, *Instruments, Methods, and Missions for Astrobiology XIV, Proc. SPIE* 8152, 81520J.

21. F. Rull, A. Sansano, E. Díaz, M. Colombo, T. Belenguer, M. Fernández, V. Guembe, et al., (2011b), A New Spectrometer concept for Mars Exploration, *Instruments, Methods, and Missions for Astrobiology XIV, Proc. SPIE* , 8152, 81520K

22. E. Díaz, A.G. Moral, C.P. Canora, G. Ramos, O. Barcos, J.A.R. Prieto, I.B. Hutchinson, et al., (2011) ExoMars Raman Laser Spectrometer Breadboard Overview, *Instruments, Methods, and Missions for Astrobiology XIV, Proc. SPIE*, **8152**, 81520L.

23. A. Wang, L.A. Haskin, et al., (2003) Development of the Mars microbeam Raman spectrometer (MMRS), *JGR*, **108**, E1, 5005.

24. T. Hirschfeld (1974) Range independence of signal in variable focus remote Raman spectrometry, *Appl. Optics,* **13**, 1435-1437.

25. S.M. Angel, T.J. Kulp, and T.M. Vess (1992) Remote Raman spectroscopy at

intermediate ranges using low-power cw lasers, *Appl. Spectrosc.* **46**, 1085-1091.

26. P.G. Lucey, T.F. Cooney, and S.K. Sharma (1998) A remote Raman analysis system for planetary landers. Abstract #1354. *Lunar Planet. Sci. XXIX*. The Lunar and Planetary Institute, Houston. http://www.lpi.usra.edu/meetings/LPSC98/pdf/1354.pdf

27. M.N. Abedin, A.T. Bradley, S. Ismail, S.K. Sharma, and S.P. Sandford (2013) Compact remote multi-sensing instrument for planetary surfaces and atmospheres characterization, *Applied Optics,***52**, 3116-3126.

28. M.N. Abedin, A.T. Bradley, S.K. Sharma, A.K. Misra, P.G. Lucey, C.S. McKay, S. Ismail, and S.P. Sandford, "Mineralogy and astrobiology detection using laser remote sensing instrument", Applied Optics, **54**, 7598-7611(2015).

29. S.K. Sharma, S.M. Angel, M. Ghosh, H.W. Hubble, and P.G. Lucey (2002) Remote pulsed laser Raman spectroscopy system for mineral analysis on planetary surfaces to 66 meters, *Appl. Spectrosc*. **56,** 699-705.

30. S.K. Sharma, P.G. Lucey, M. Ghosh, H.W. Hubble, and K.A. Horton (2003a) Stand-off Raman spectroscopic detection of minerals on planetary surfaces, *Spectrochim. Acta, A***59**, 2391-2407.

31. S.K. Sharma, J.N. Porter, A.K. Misra, H.W. Hubble, and P. Menon (2003b) Portable standoff Raman and Mie-Rayleigh lidar for cloud, aerosol, and chemical monitoring, *Proc. SPIE* **5154,** 1-14.

32. S.K. Sharma, S. Ismail**,** S.M. Angel**,** P.G. Lucy**,** C.P. McKay**,** A.K. Misra, P.J. Mouginis-Mark, H. Newsom, U.N. Singh, and G. J. Taylor (2004) Remote Raman and Laser-induced Fluorescence (RLIF) Emission Instrument for Detection of Minerals, organic and Biogenic Materials on Mars to 100 Meters Radial Distance, *Proc. SPIE* **5660**, 128-138.

33. S.K. Sharma, A. Wang, L.A. Haskin (2005b) Remote Raman Measurements of Minerals with Mars Microbeam Raman Spectrometer (MMRS), *Lunar Planet. Sci.Conf.* **XXXVI**, Abstract. #1524, http://www.lpi.usra.edu/meetings/lpsc2005/pdf/1524.pdf

34. S.K. Sharma, A. Misra, and P. Lucey (2006a) A combined remote Raman and fluorescence spectrometer system for detecting inorganic and biological materials, *Proc. SPIE*, **6409**, 6409K/1–6409K/9.

35. S.K. Sharma, A.K. Misra, P.G. Lucey, S.M. Angel, and C.P. McKay (2006b) Remote pulsed Raman spectroscopy of inorganic and organic materials to a radial distance of 100 meters, *Appl. Spectrosc.*,**60**, 871-876.

36. S.K. Sharma, A.K. Misra, P.G. Lucey, R.C. Wiens and S.M. Clegg (2007a) Combined Remote LIBS and Raman Spectroscopy of Sulfur-Containing Minerals, and Minerals Coated with Hematite and Covered with Basaltic Dust at 8.6 m, *Spectrochim. Acta A*, **68**, 1036-1045.

37. S.K. Sharma, (2007b) New trends in telescopic remote Raman spectroscopic instrumentation, *Spectrochimica Acta part A*, **68**, 1008-1022.

38. S.K. Sharma and A.K. Misra (2008) Remote Raman spectroscopic detection of inorganic, organic and biological materials to 100 m and more, *Proc. 2nd International Conference on Perspectives in Vibrational Spectroscopy (ICOPVS 2008)*, American Institute of Physics, **1075 (1),** doi:10.1063/1.3046223.

39. A.K. Misra, S.K. Sharma, C.H. Chio, P.G. Lucey, and B. Lienert (2005) Pulsed remote Raman system for daytime measurements

of mineral spectra, *Spectrochim Acta, A* **61**, 2281-2287.

40. A.K. Misra, S.K. Sharma, and P.G. Lucey (2006) Remote Raman spectroscopic detection of minerals and organics under illuminated condition from 10 m distance using a single 532 nm laser pulse, *Appl. Spectrosc.***60**, 223-228.

41. A.K. Misra, S.K. Sharma, D.E. Bates, T.E. Acosta (2010) Compact standoff Raman system for detection of homemade explosives, *Proc. SPIE,***7665**, 76650U, DOI: 10.1117/12.849850.

42. A.K. Misra, S.K. Sharma, T.E. Acosta, and D.E. Bates (2011a) Detection of Chemicals with Standoff Raman spectroscopy, *Spectroscopy, Special Issue: Defense & Homeland Security*, pp. 18-23 (April 1). Available on line: http://www.spectroscopyonline.com/spectroscopy/article/articleDetail.jsp?id=719325

43. A.K. Misra, S.K. Sharma, T.E. Acosta, D.E. Bates (2011b) Compact remote Raman and LIBS system for detection of minerals, water, ices, and atmospheric gases for planetary exploration, *Next-Generation Spectroscopic Technologies IV*, *Proc. SPIE* , **8032**, 80320Q-80320Q-12.

44. A.K. Misra, S.K. Sharma, T.E. Acosta, J.N. Porter and D.E. Bates, (2012a) Single pulse remote Raman detection of chemicals from 120 m distance during daytime, *Applied Spectroscopy, Appl. Spectrosc.***66**, 1279-1285.

45. T.E. Acosta-Maeda, A.K. Misra, L.G. Muzangwa, G. Berlanga, D. Muchow, J. Porter, and S.K. Sharma, Remote Raman measurements of minerals, organics, and inorganics at 430 m range, Applied Optics 55(36) 10283-10289 (2016)

46. M.N. Abedin, A.T. Bradley, A.K. Misra, S.K. Sharma, and J. Osmundsen, Ultra-Compact Raman spectrograph for planetary surface inspection, 47th Lunar and Planetary Science Conference, Abstract # 1085, 2016.

47. X.B. Wang, Z.X. Shen, S.H. Tang, and M.H. Kuok, Near infrared excited micro-Raman spectra of 4:1 methanol–ethanol mixture and ruby fluorescence at high pressure, J. Appl. Phys. 85, 8011-8017 (1999).

48. C.S. Garcia, M.N. Abedin, S. Ismail, S.K. Sharma, A.K. Misra, S.P. Sandford, and H. Elsayed-Ali, Design and build a compact Raman sensor for identification of chemical composition, Proc. SPIE 6943, 69430I (2008).

49. http://www.chem.ualberta.ca/~mccreery/images/Photo%20raman%20intensity%20standard/napthalene.jpg.

50. A.L. Jenkins, R.A. Larsen, and T.B. Williams, Characterization of amino acids using Raman spectroscopy, Spectrochimica Acta Part A 61, 1585-1594 (2005).

51. J. Blacksberg, G.R. Rossman, and A. Gleckler, Time-resolved Raman spectroscopy for in situ planetary mineralogy, Applied Optics, 49, (2010).

52. A. Pawlukojc, K. Holderna-Natkaniec, G. Bator, and I. Natkaniec, L-glutamine: Dynamical properties investigation by means of INS, IR, Raman, 1H NMR, and DFT techniques, Chemical Physics 443, 17-25 (2014).

53. T.E. Acosta-Maeda, A.K. Misra, P.J. Gasda, and S.K. Sharma, Stand-off detection of amino acids and organics using a compact remote Raman instrument, Abstract # 2331, 45thLunar and Planetary Science Conference (2014).